International Journal of Control

ISSN: 0020-7179 (Print) 1366-5820 (Online) Journal homepage: www.tandfonline.com/journals/tcon20

Open-loop step response IMC-based tuning of PIDA controllers

Francesco Campregher, Marco Milanesi, Michele Schiavo & Antonio Visioli

To cite this article: Francesco Campregher, Marco Milanesi, Michele Schiavo & Antonio Visioli (16 Mar 2026): Open-loop step response IMC-based tuning of PIDA controllers, International Journal of Control, DOI: 10.1080/00207179.2026.2643626

To link to this article: https://doi.org/10.1080/00207179.2026.2643626

Published online: 16 Mar 2026.

INTERNATIONAL JOURNAL OF CONTROL
https://doi.org/10.1080/00207179.2026.2643626

Taylor & Francis
Taylor & Francis Group

Open-loop step response IMC-based tuning of PIDA controllers

Francesco Campregher[a,b], Marco Milanesi[a], Michele Schiavo[a] and Antonio Visioli[a]

[a]Dipartimento di Ingegneria Meccanica e Industriale, University of Brescia, Brescia, Italy; [b]Polytechnic of Bari, Bari, Italy

ABSTRACT

In this paper, we propose a tuning procedure for Proportional-Integral-Derivative-Acceleration (PIDA) controllers. In particular, starting from a third-order-plus-dead-time process transfer function estimated by evaluating an open-loop step response, the controller is tuned by means of an Internal Model Control (IMC) approach where the controller transfer function is reduced by truncating its Maclaurin series. Measurement noise is mitigated through the design of appropriate low-pass filters. A comparison with a previously devised open-loop Haalman tuning method based on pole-zero cancellation and with a similar tuning technique for a PID controller is performed. Further, experimental results with a temperature control laboratory are shown, demonstrating the practical applicability of these controllers in process control contexts.

ARTICLE HISTORY
Received 8 September 2025
Accepted 6 March 2026

KEYWORDS
PIDA controllers; tuning; internal model control; experimental results

1. Introduction

Although Proportional-Integral-Derivative (PID) controllers have been proven to be very effective for many industrial processes, there is always the effort by the researchers to provide new tuning rules or additional functionalities in order to increase their performance by keeping at the same time their ease of use. In fact, it is recognised that any advancement in this field should take into account the main reasons for the success of PID controllers: their simple structure, their intuitiveness and the availability of a wide variety of tuning rules that facilitate their overall design (O'Dwyer, 2006). Thus, the possible increment of the performance achieved by considering a new methodology should not come at the expense of worsening the cost/benefit ratio of standard PID controllers.

In this context, there has been an effort in the investigation of high-order controllers, such as, for example, fractional-order PID controllers, which can be considered as a relatively simple approach to design controllers with many poles and zeros (Monje et al., 2008; Tepljakov et al., 2018). Recently, the use of Proportional-Integral-Derivative-Acceleration (PIDA) controllers, also known as Proportional-Integral-Double-Derivative (PIDD or PIDD2) controllers has also emerged as a valid option. Actually, in Milanesi et al. (2022, 2025) an evolutionary approach has been employed to tune such controllers for the set of benchmark processes proposed in Åström and Hägglund (2000) and it has emerged that the main performance improvements can be obtained with (self-regulating) high-order processes. The effectiveness of these controllers for integral processes has also been shown (Huba, 2019; Huba et al., 2023a, 2023b; Huba et al., 2024). Remarkably, experimental results related to motion and temperature control problems are included in Bistak et al. (2023) and Huba et al. (2023b, 2024), showing the potentiality of PIDA controllers in industry. In general, the presence of additional zeros can be exploited to increase the system bandwidth without decreasing the system robustness.

However, the additional (acceleration) control action requires the development of new tuning rules, as the manual tuning can be more complex and the physical meaning of the additional parameters might not be fully intuitive (Ferrari & Visioli, 2022). Furthermore, the possible amplification of the measurement noise should be carefully considered and the low-pass filters should be integrated into the design of the overall controller. Indeed, it is well known that, in process control, the derivative action is not employed mainly because of the noise issue. It is therefore essential to demonstrate that the double derivative action can be used in practice by suitably adding low-pass filters, whose design should not be complex from the user perspective.

Since Internal Model Control (IMC) has been proven to be a very effective design methodology that is still widely investigated (see, for example, Aryan et al., 2025; Biswas et al., 2025), it is sensible to use this approach also

CONTACT Antonio Visioli antonio.visioli@unibs.it Dipartimento di Ingegneria Meccanica e Industriale, University of Brescia, Via Branze 38, Brescia I-25123, Italy

for PIDA controllers. In this context, a design methodology has been recently proposed in Huba and Vrancic (2021) where the process model is assumed to have multiple poles in the same location. Then, in Visioli and Sanchez-Moreno (2024a, 2024b) a closed-loop relay-feedback experiment is exploited to determine a high-order process model with the application of the so-called n-shifting technique (Sanchez et al., 2021; Visioli & Sanchez-Moreno, 2023). Differently, an open-loop tuning procedure has been proposed in Campregher et al. (2024) where a Third-Order-Plus-Dead-Time (TOPDT) process model is obtained from an open-loop process step response (Sanchis & Peñarrocha-Alós, 2022, 2023) and then a generalised Haalman method is employed (Åström & Hägglund, 2006). It consists of cancelling all the poles of the process with the zeros of the controller and then of selecting the proportional gain in order to achieve a desired maximum sensitivity. A classic IMC procedure has been applied in Kumar and Hote (2021) for a DC-DC boost converter. In this case, because of the model of the process, the resulting controller is of PIDA type, but it has to be noted that the process has no dead time.

In this paper, we propose to use the IMC-based approach with a TOPDT process model estimated by evaluating an open-loop step response. In particular, once the process model has been determined, the IMC controller transfer function is calculated with the design parameters that are selected in order to handle the trade-off between aggressiveness and robustness, that is, in order to obtain a desired value of the maximum sensitivity. The controller transfer function is then approximated as a PIDA controller (with the low-pass filters on the derivative and acceleration actions) by suitably truncating its Maclaurin series expansion.

It is worth stressing that, in general, the IMC approach mainly addresses the set-point following task because it is based on pole-zero cancellation. For lag-dominant processes this yields sluggish transients in the load disturbance rejection task, but this is not an issue in this paper because, as already mentioned, we consider high-order processes, with a relatively high apparent dead time (with respect to the dominant time constant). The effectiveness of the procedure is demonstrated with simulation results but also with experimental results related to a temperature control problem. Although they have been obtained with a simple laboratory equipment, they are very relevant because they show that suitably designed PIDA controllers can be used in process control applications despite the presence of a significant measurement noise.

Summarising, the main contributions of the paper can be outlined as follows:

- a new open-loop tuning procedure is proposed for PIDA controllers, where the user can select a desired trade-off between aggressiveness and robustness;
- a comparison with other tuning method is provided; although the comparison is based on examples and it is therefore not exhaustive, it can be used to conclude that the method provides better results with respect to a similarly designed PID controller;
- experimental results, are given, demonstrating that the proposed approach is effective in practical applications.

The paper is organised as follows. The control problem is formulated in Section 2. The tuning procedure is outlined in Section 3. Illustrative simulation results are shown in Section 4, where a comparison with the generalised Haalman tuning and with PID controllers tuned by using the same open-loop approaches is performed, and discussed in Section 5. Conclusions are finally drawn in Section 6.

2. Problem formulation

We consider the standard unity-feedback control system shown in Figure 1, where P is the process, C is the controller, y is the process variable, y_{sp} is the set-point signal, u is the control variable, d is the load disturbance signal and n is the measurement noise signal.

The process P is assumed to be self-regulating (i.e. asymptotically stable) and its model is expressed as a transfer function

$$\tilde{P}(s) = p_m(s)e^{-Ls} \tag{1}$$

where $p_m(s)$ is the delay-free and minimum-phase part of the process. The PIDA controller transfer function is expressed as

$$C(s) = K_p\left(1 + \frac{1}{T_i s} + \frac{T_d s}{\frac{T_d}{N}s + 1} + \frac{T_a s^2}{\left(\frac{T_a}{N}s + 1\right)^2}\right)$$

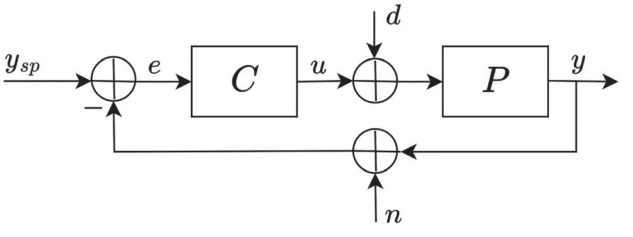

Figure 1. The considered standard unity-feedback control system.

$$\times \frac{1}{(T_f s+1)^2} \tag{2}$$

where K_p is the proportional gain, T_i is the integral time constant, T_d is the derivative time constant, T_a is the acceleration time constant, and N is the parameter of the low-pass filters that are applied to the derivative and acceleration actions to make the controller proper and avoid the amplification of the measurement noise. Note that the same parameter is used for both filters in order to simplify the computation of the controller. Finally, in order to make the noise filtering more effective, an additional second-order low-pass filter with time constant T_f is applied to the controller output.

For the purpose of the controller design, its transfer function can be expressed as

$$C(s) = \tilde{C}(s)H(s) \tag{3}$$

where $\tilde{C}(s)$ is the PIDA part and $H(s)$ is the second-order output filter.

The aim of the proposed methodology is to find the values of all the controller parameters given a process model estimated by evaluating an open-loop step response, as it is typically done in industry (Åström & Hägglund, 2006; Visioli, 2006).

3. Tuning method

Given that the PIDA controller (2) has four zeros (and six poles, including those of the output filter), it is sensible to use a methodology to estimate a high-order transfer function of the process by evaluating an open-loop step response. Given that simplicity in experimentation and calculation is essential in process industry applications, we employ the method presented in Sanchis and Peñarrocha-Alós (2022) for the determination of a TOPDT model. It consists of determining the time instants t_5, t_{35} and t_{85} when the process step response achieves, respectively, 5%, 35% and 85% of its final value. Then, the transfer function is determined as:

$$\tilde{P}(s) = \frac{K}{(1+\tau s)\left(1+\frac{(1-\alpha)\theta}{2}s\right)^2} e^{-\alpha\theta s} \tag{4}$$

where the gain K is the ratio of the steady-state variation of the output to that of the input, and the other parameters are calculated as

$$\begin{aligned} \theta &= 1.3t_{35} - 0.29t_{85} \\ \tau &= 0.67(t_{85} - t_{35}) \\ \alpha &= 0.598 + 0.4799\frac{t_5}{\theta} - \frac{0.41}{\left(\frac{t_5}{\tau}\right)^{0.6}} \end{aligned} \tag{5}$$

Thus, in (1) we have that

$$p_m(s) = \frac{K}{a_3 s^3 + a_2 s^2 + a_1 s + 1} \tag{6}$$

where

$$\begin{aligned} a_3 &= \theta^2\tau\left(\frac{\alpha}{2} - \frac{1}{2}\right)^2 \\ a_2 &= \theta^2\left(\frac{\alpha}{2} - \frac{1}{2}\right)^2 - 2\theta\tau\left(\frac{\alpha}{2} - \frac{1}{2}\right) \\ a_1 &= \tau - 2\theta\left(\frac{\alpha}{2} - \frac{1}{2}\right) \end{aligned} \tag{7}$$

and

$$L = \alpha\theta. \tag{8}$$

Once the process model is obtained, the PIDA controller can be designed by first selecting the desired closed-loop transfer function as

$$F(s) = \frac{Y(s)}{Y_{sp}(s)} = \frac{e^{-Ls}}{(\lambda s+1)^r}. \tag{9}$$

Here it appears that the design parameters r and λ have a clear physical meaning and can be therefore chosen in order to handle the trade-off between aggressiveness and robustness and control effort. In particular, for a given value of r, a reduction of the time constant λ implies a faster response (with an increment of the control effort). Similarly, for a given value of λ, a reduction of r implies again a faster response (Visioli & Sanchez-Moreno, 2023, 2024a).

The definition of (9) implies that the controller transfer function is

$$C(s) = \frac{F(s)}{\tilde{P}(s)[1-F(s)]} = \frac{p_m^{-1}(s)}{(\lambda s+1)^r - e^{-Ls}}. \tag{10}$$

This can be expanded as a truncated Maclaurin series:

$$\begin{aligned} C(s) = \frac{f(s)}{s} \cong \frac{1}{s}\Bigg[f(0) + f^{(1)}(0)s + \frac{f^{(2)}(0)}{2}s^2 \\ + \frac{f^{(3)}(0)}{6}s^3 + \frac{f^{(4)}(0)}{24}s^4\Bigg]. \end{aligned} \tag{11}$$

On the other side, the PIDA controller transfer function (without the output filter) can also be expressed as

$$\begin{aligned} \tilde{C}(s) \cong \frac{1}{s}\Bigg[\frac{K_p}{T_i} + K_p s + K_p T_d s^2 + K_p\left(T_a - \frac{T_d^2}{N}\right)s^3 \\ - K_p\left(\frac{2T_a^2}{N} - \frac{T_d^3}{N^2}\right)s^4\Bigg]. \end{aligned} \tag{12}$$

By equating (12) and (11), we can therefore obtain the values of the controller parameters. Note that the truncation of the series implies that a pole-zero cancellation is not obtained. Further, the output low-pass filter is not explicitly included because, in this way, the analytical expressions can be easily determined. Its time constant can therefore finally be selected in order to manage the trade-off between an effective noise filtering and the set-point transient performance. In fact, increasing the time constant yields a better noise filtering but also a decrement of performance in terms of an additional phase lag, that is, an increased overshoot in the set-point step response with respect to the expected results, that is, the step response of (9) (see Section 4). Taking this into account, a sensible choice is to select T_f as a fraction of the inverse of the gain crossover frequency ω_{gc} of the loop transfer function, that is:

$$T_f = \frac{k_f}{\omega_{gc}} \tag{13}$$

where ω_{gc} is the gain crossover frequency, that is, the solution of the equation

$$\left|\tilde{C}(j\omega_{gc})\tilde{P}(j\omega_{gc})\right| = 1. \tag{14}$$

An initial choice can be $k_f = 0.01$ so that the filter does not virtually affect the dynamics of the designed controller even if its filtering action is essential (see Section 4). Then, if with this choice the control variable is still too noisy, the value of T_f can be conveniently increased until the noise level is acceptable. In any case, it is worth stressing that, in a digital implementation of the controller, the choice of the sampling period should take into account also the additional filter.

4. Simulation results

Illustrative simulation results related to a fourth- and a eighth-order process are presented in this section. In both cases, unit set-point and load disturbance step responses are evaluated (in all the plots, the set-point signal is shown as a dashed line). Measurement noise, simulated by adding to the process output a random number between −0.1 and 0.1, is also considered in all the presented results.

The proposed methodology is compared with a PID controller tuned by using the same IMC-based approach by starting from a second-order-plus-dead-time model obtained by applying the iterative method based on the integrals of the open-loop set-point step response signals proposed in Veronesi et al. (2024). Further, the method is compared with a PIDA and a PID controller tuned by applying the generalised Haalman technique proposed in Campregher et al. (2024). In order to provide a fair comparison, we select in all cases similar values of the maximum sensitivity M_s, which is defined as

$$M_s = \max_{\omega\in[0,+\infty)} \left|\frac{1}{1 + C(j\omega)P(j\omega)}\right| \tag{15}$$

Further, again to provide a fair comparison, the time constant of the output low-pass filters for these controllers is selected so that the noise amplification is as similar as possible, but without decreasing the performance too much. In all cases the controller has been discretised with a sampling period of 0.001 s that is sufficiently small taking into account the control system bandwidth. The simulations have been performed with a fixed integration time step of 10^{-5} s.

4.1 Fourth-order process

As a first example, we consider the process

$$P_1(s) = \frac{1}{(s+1)^4}. \tag{16}$$

The evaluation of the open-loop step response yields the following parameters of the TOPDT model: $K = 1$, $L = 2.159$, $\alpha = 0.382$, $\tau = 2.037$ (see (5)), yielding

$$P_1(s) = \frac{1}{0.90s^3 + 3.16s^2 + 3.37s + 1} e^{-0.83s} \tag{17}$$

where the poles are at $\{-1.5, -1.5, -0.49\}$. Then, by selecting $r = 3$ and $\lambda = 1$, the IMC-based tuning procedure can be applied, yielding the parameters shown in Table 1. The corresponding transfer function is

$$C(s) = \frac{1.0794(s + 0.6197)(s + 0.4794)(s^2 + 1.298s + 0.5265)}{s(s + 0.9329)^2(s + 0.7421)} \tag{18}$$

Note that there is not a pole-zero cancellation because of the truncation of the Mclaurin series. The resulting value of the maximum sensitivity is $M_s = 1.46$, which is a typical satisfactory value for ensuring the robust stability of the system (Åström & Hägglund, 2006).

Table 1 shows also the parameters of the PID controller designed by applying the same IMC-based method with the same values of r and λ (and therefore with virtually the same value of M_s) and of the PIDA and PID controllers designed by applying the generalised Haalman

Table 1. Results obtained for Example 1.

Controller	K_p	T_i	T_d	T_a	N	T_f	M_s
PIDA IMC-based	0.70	2.67	0.38	0.30	0.28	0.04	1.46
PID IMC-based	0.56	2.30	0.19	–	0.09	1.22	1.49
PIDA – Haalman	1.46	3.37	0.94	0.27	10	0.91	1.47
PID – Haalman	1.02	2.88	0.72	–	10	2.81	1.47

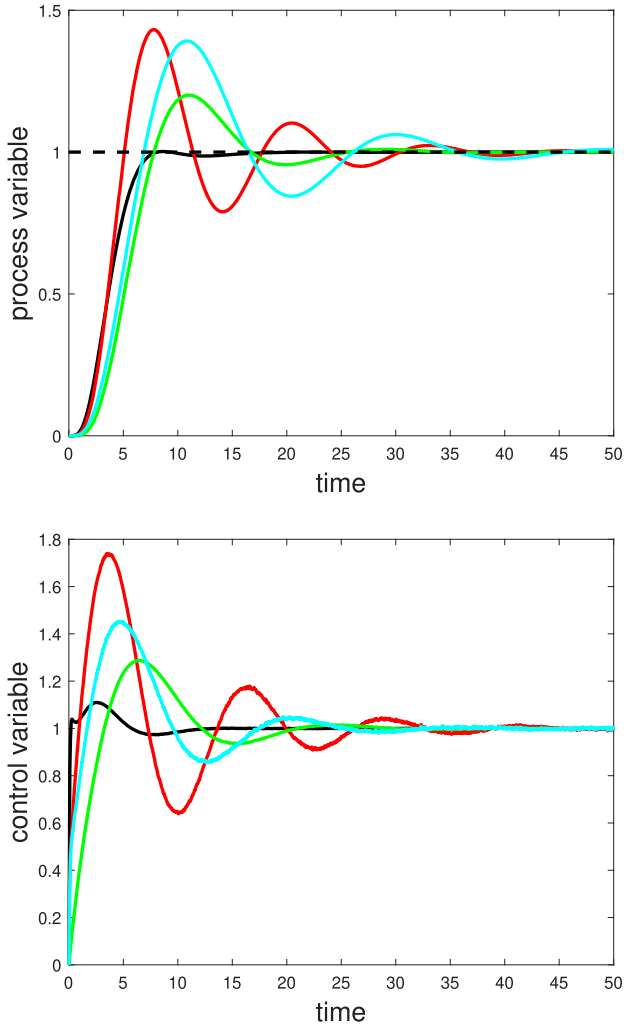

Figure 2. Set-point step response for Example 1. Top: process variable. Bottom: control variable. Black line: IMC-based PIDA controller. Green line: IMC-based PID controller. Red line: PIDA controller tuned with the generalised Haalman method. Cyan line: PID controller tuned with the generalised Haalman method.

tuning proposed in Campregher et al. (2024). The set-point step responses of all the considered cases are plotted in Figure 2. Note that the time scale of the control variable is different from that of the process variable in order to better highlight the first part of the transient response. In order to evaluate the performance quantitatively, the integrated absolute error, defined as

$$IAE = \int_0^\infty |e(t)|\,\mathrm{d}t, \tag{19}$$

and the total variation defined as

$$TV = \sum_{k=1}^{\infty} |u(k) - u(k-1)|, \tag{20}$$

(where k is the sampling instant) have been calculated in the different cases. Note that these performance indexes

Table 2. Performance indexes obtained for Example 1.

Controller	IAE_{sp}	TV_{sp}	IAE_{ld}	TV_{ld}
PIDA IMC-based	4.00	1.73	3.96	1.44
PID IMC-based	7.86	2.56	7.10	2.30
PIDA – Haalman	7.89	6.36	6.10	5.29
PID – Haalman	9.18	10.6	7.95	10.3

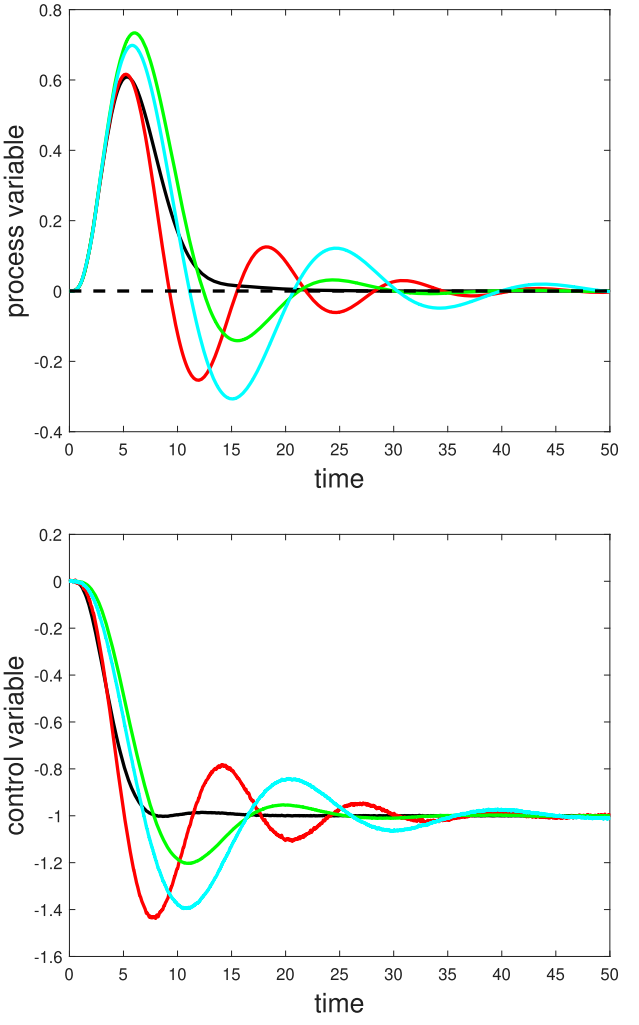

Figure 3. Load disturbance step response for Example 1. Top: process variable. Bottom: control variable. Black line: IMC-based PIDA controller. Green line: IMC-based PID controller. Red line: PIDA controller tuned with the generalised Haalman method. Cyan line: PID controller tuned with the generalised Haalman method.

are the most typical ones even if some modifications have been proposed (Huba & Vrancic, 2021). The resulting values are shown in Table 2, where IAE_{sp} and TV_{sp} are related to the set-point step response and IAE_{ld} and TV_{ld} are related to the load disturbance step response. The load disturbance step responses of all the considered cases are plotted in Figures 2 and 3, respectively.

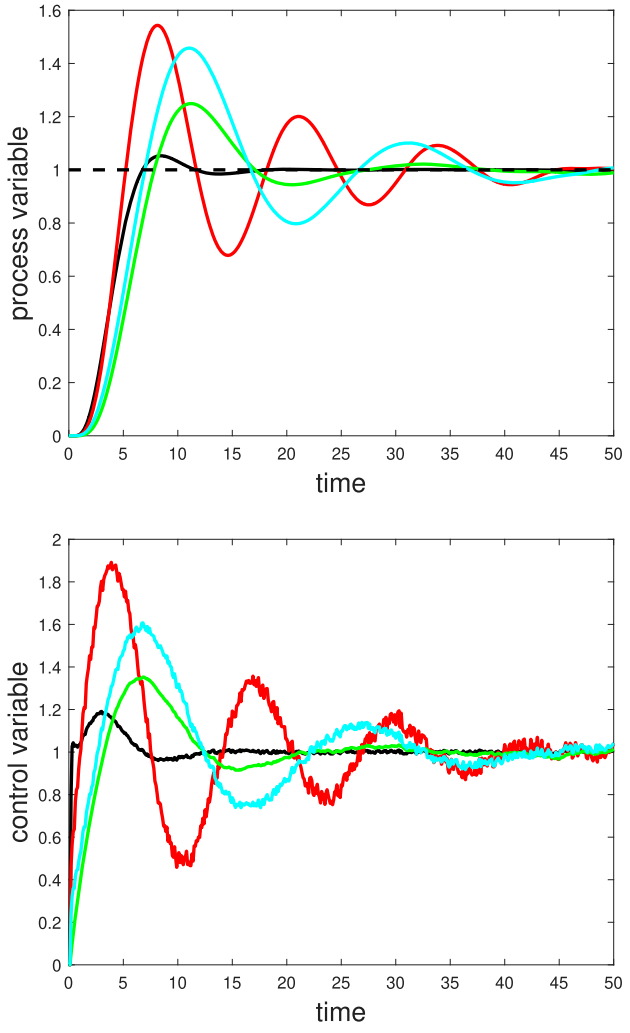

Figure 4. Set-point step response for Example 1 with a sampling period of 0.1 s. Top: process variable. Bottom: control variable. Black line: IMC-based PIDA controller. Green line: IMC-based PID controller. Red line: PIDA controller tuned with the generalised Haalman method. Cyan line: PID controller tuned with the generalised Haalman method.

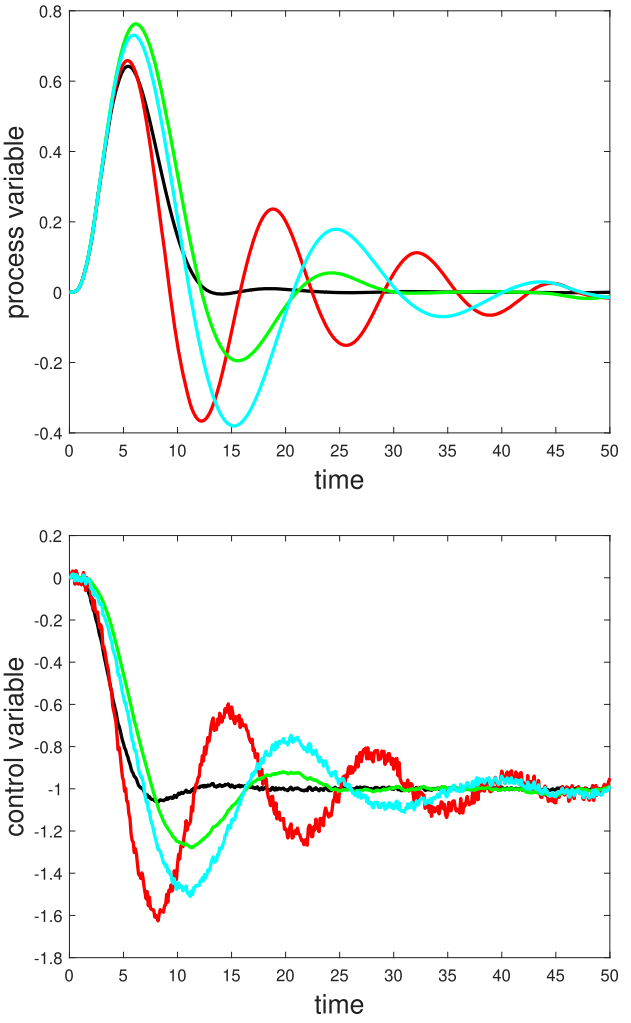

Figure 5. Load disturbance step response for Example 1 with a sampling period of 0.1 s. Top: process variable. Bottom: control variable. Black line: IMC-based PIDA controller. Green line: IMC-based PID controller. Red line: PIDA controller tuned with the generalised Haalman method. Cyan line: PID controller tuned with the generalised Haalman method.

For the sake of evaluating the role of the sampling period, the same simulations as before has been performed with a sampling period of 0.1 s. Results are shown in Figures 4 and 5, where it appears that the proposed method is effective in filtering the noise even with lower sampling periods.

In order to better understand the role of the output filter time constant, different simulations have been done by changing the value of k_f. Results (only for the set-point response, for the sake of brevity) for $k_f = \{0.01, 0.05, 0.1\}$ are shown in Figure 6, using the same measurement noise. They are compared with the results obtained without the output filter. In this latter case the noise-free case has been considered because, otherwise, the resulting control variable would be too noisy. The role of the filter time constant can be observed. In general, it appears that the filter, although essential, can be set in such a way that the overall dynamics is not significantly affected by it, thanks to the other low-pass filters applied to the derivative and acceleration action.

Finally, in order to better understand the role of the tuning parameters λ and r, the results obtained with the PIDA controller by fixing the value of $r = 3$ and by changing the value of λ in the range from 0.4 to 1.2 are shown in Figures 7 and 8 for the set-point and load disturbance responses, respectively. The corresponding values of the parameters are shown in Table 3, where it appears that the increment of λ yields a decrement of all the parameters of the controller, including the acceleration parameter T_a. Thus, the role of λ in handling the trade-off between aggressiveness and control effort can be easily understood. On the other hand, the results obtained,

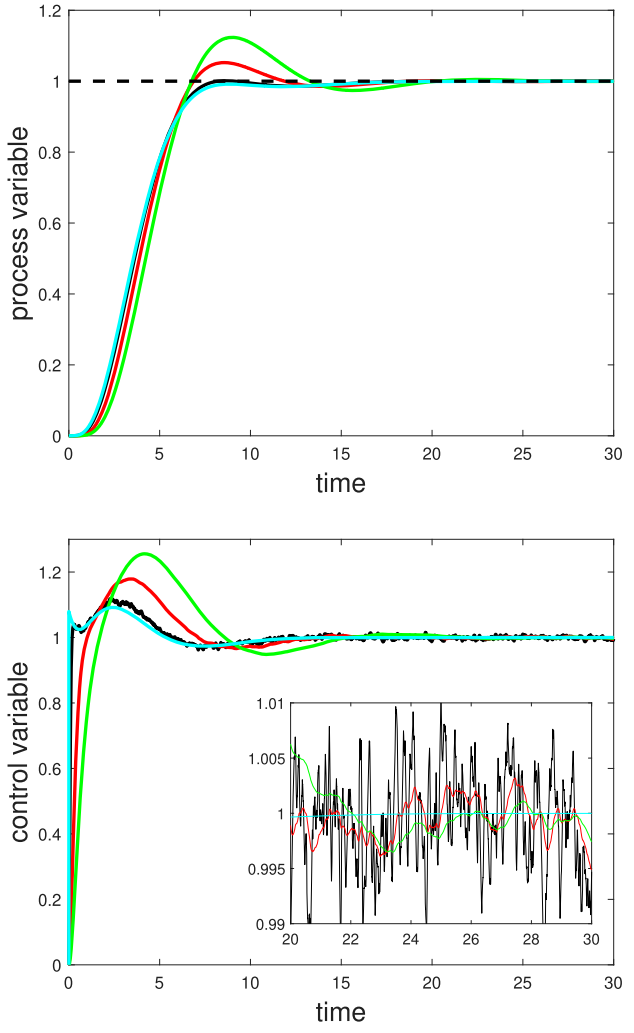

Figure 6. Set-point step response for Example 1 (IMC-based PIDA controller) with different values of k_f. Top: process variable. Bottom: control variable. Black line: $k_f = 0.01$. Red line: $k_f = 0.05$. Green line: $k_f = 0.1$. Cyan line: no filter (and no noise).

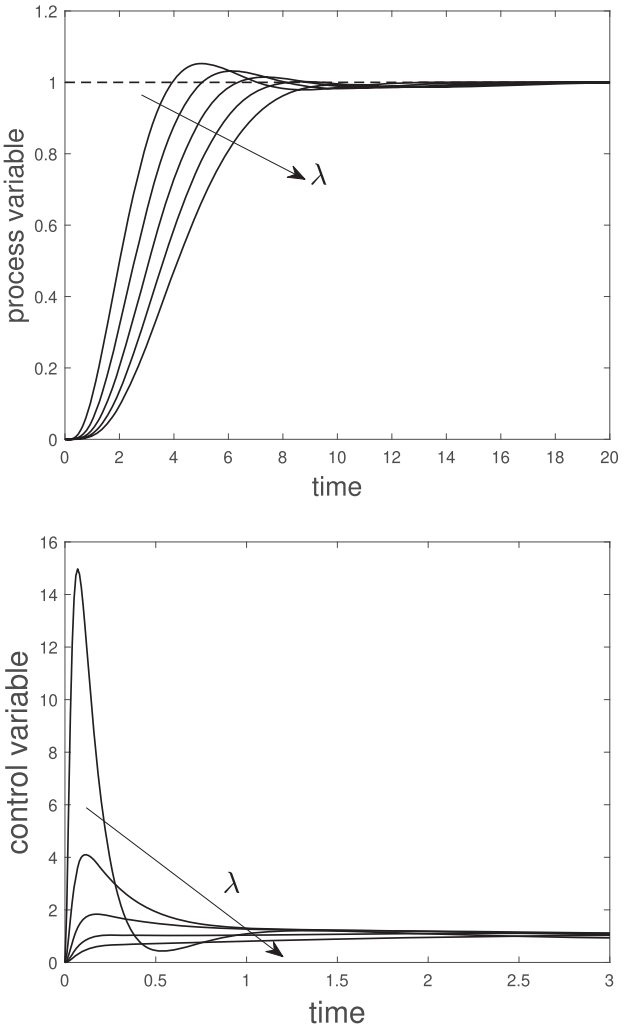

Figure 7. Set-point step response for Example 1 (PIDA controller) with $r = 3$ and $\lambda = 0.4, 0.6, 0.8, 1.0, 1.2$. Top: process variable. Bottom: control variable.

again with the PIDA controller, by fixing $\lambda = 0.6$ and by selecting $r = 3, 4, 5$ are shown in Figures 9 and 10, where the physical meaning of r can be observed. The controller parameters are shown in Table 4, where it appears that, as for λ, an increment of r implies a decrement of the controller's parameters.

4.2 Eighth-order process

In the second example we increase the number of multiple poles in the process, that is,

$$P_2(s) = \frac{1}{(s+1)^8}. \tag{21}$$

which is approximated by a TOPDT model with $K = 1$, $L = 5.51$, $\alpha = 0.61$, and $\tau = 2.87$, that is,

$$P_2(s) = \frac{1}{3.304s^3 + 7.304s^2 + 5.01s + 1} e^{-3.36s} \tag{22}$$

where the poles are at $\{-0.93, -0.93, -0.35\}$. In this case the IMC parameters have been selected as $r = 3$ and $\lambda = 1$, and the resulting value of the maximum sensitivity for the corresponding PIDA controller is $M_s = 1.77$. The parameters of the PIDA controller are shown in Table 5. The corresponding transfer function is

$$C(s) = \frac{5.5681(s + 1.37)(s + 0.3185)}{(s^2 + 0.7849s + 0.221)} \frac{}{s(s + 1.568)^2(s + 1.388)}. \tag{23}$$

Table 5 also shows the parameters of the other controllers used for comparison. In each case, as for the previous example, the filter time constants has been adjusted in order to have a similar filtering of the measurement noise without being too detrimental for the performance, namely, without a too large overshoot. The set-point step

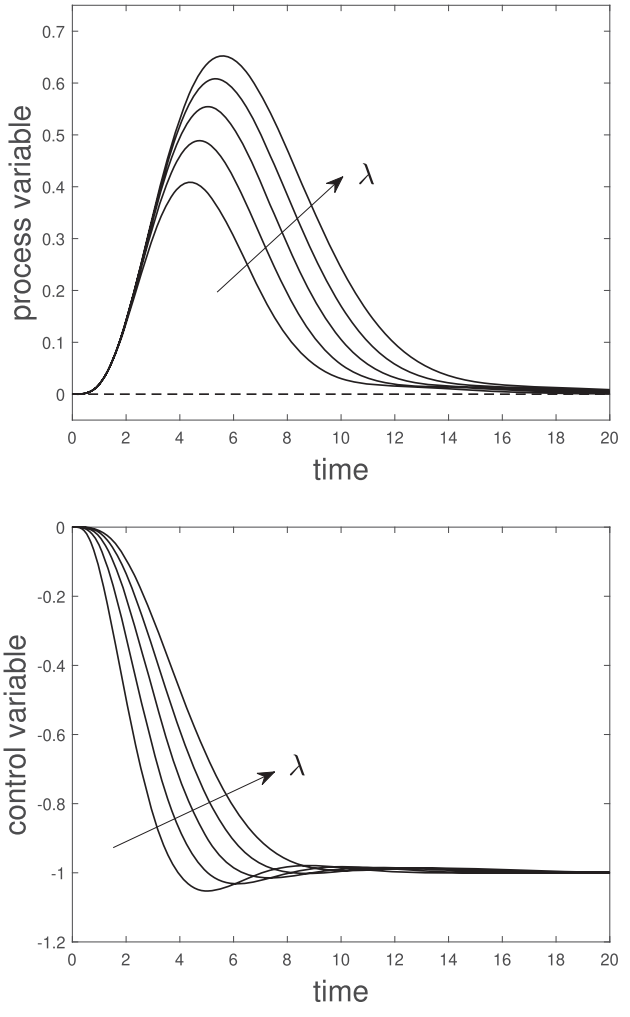

Figure 8. Load disturbance step response for Example 1 (PIDA controller) with $r = 3$ and $\lambda = 0.4, 0.6, 0.8, 1.0, 1.2$. Top: process variable. Bottom: control variable.

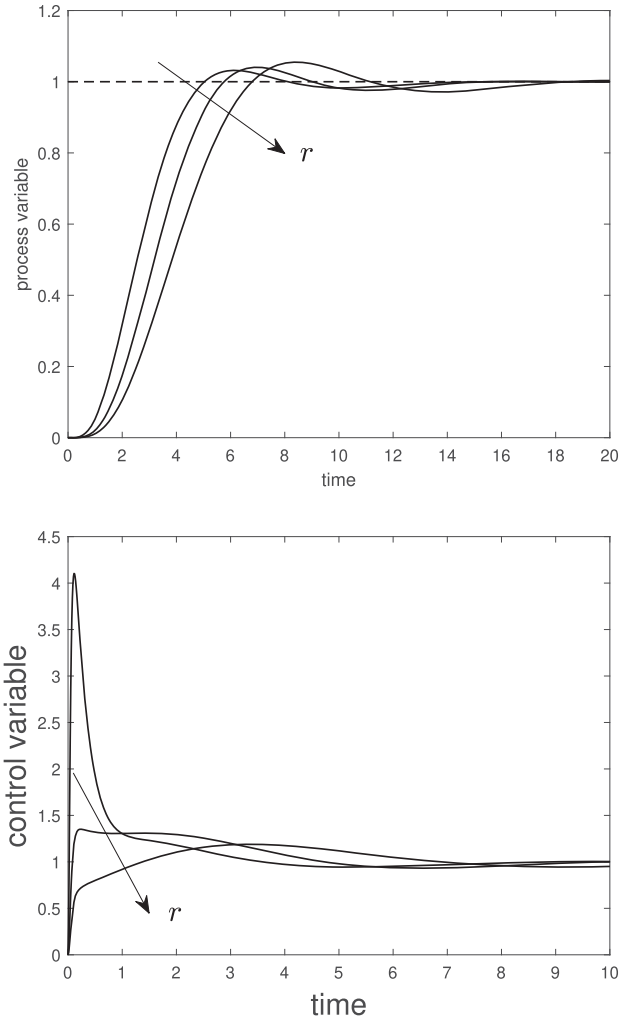

Figure 9. Set-point step response for Example 1 (PIDA controller) with $\lambda = 0.6$ and $r = 3, 4, 5$. Top: process variable. Bottom: control variable.

responses are plotted in Figure 11, while the load disturbance step responses are shown in Figure 12. The performance indexes are shown in Table 6.

4.3 Discussion

From the presented results, some considerations can be made by taking into account both performance indexes (Bošković et al., 2020). In both the presented cases the IMC-based PIDA controller improves the performance with respect to the other ones by providing a smaller IAE and a smaller TV at the same time. In fact, with respect to the Haalman tuning (both for PIDA and PID controllers), the main advantage of the proposed IMC-based approach is that the filters of the derivative and acceleration action are integrated in the controller design. Thus, the effective filtering actions of these two low-pass filters allows the use of a second-order filter at the controller's output with a time constant that can be selected sufficiently small to filter the noise appropriately without introducing a significant phase lag in the system. Conversely, fixing $N = 10$ in the Haalman method implies that a stronger

Table 3. Controller parameters for different values of λ for Example 1.

Value of λ	K_p	T_i	T_d	T_a	N	M_s	IAE_{sp}	TV_{sp}	IAE_{ld}	TV_{ld}
0.4	1.63	3.30	0.86	0.47	2.28	1.64	2.23	30.7	2.02	1.15
0.6	1.18	3.09	0.70	0.45	1.05	1.55	2.75	7.33	2.62	1.10
0.8	0.89	2.88	0.54	0.39	0.56	1.50	3.28	2.74	3.22	1.06
1.0	0.70	2.67	0.38	0.30	0.28	1.46	3.83	1.30	3.81	1.03
1.2	0.56	2.47	0.21	0.20	0.10	1.44	4.42	1.14	4.40	1.01

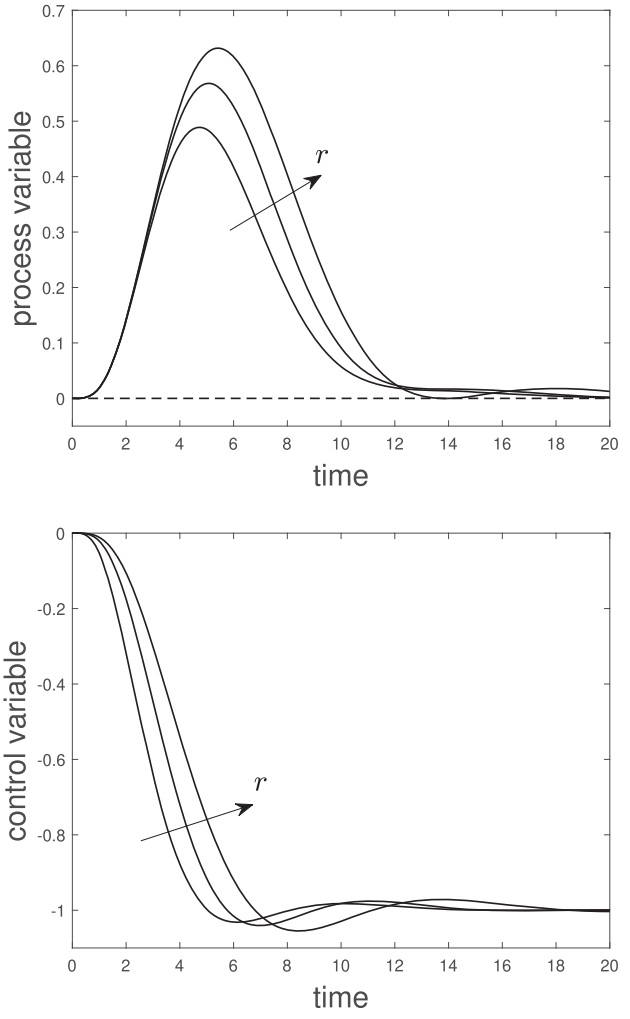

Figure 10. Load disturbance step response for Example 1 (PIDA controller) with $\lambda = 0.6$ and $r = 3, 4, 5$. Top: process variable. Bottom: control variable.

filtering action is necessary at the controller's output and this implies the occurrence of oscillations in the step responses. Thus, the most significant comparison of the proposed method should be done with the corresponding IMC-based PID controller. In this context we have that, for the fourth-order system, the IAE is reduced of 49% for the set-point step response and of 44% for the load disturbance step response, while the TV is reduced of 32% and 37%, respectively. Similar results are achieved for the eighth-order system, where the IAE is reduced of 32% for

Table 5. Results obtained for Example 2.

Controller	K_p	T_i	T_d	T_a	N	T_f	M_s
PIDA IMC-based	0.85	5.42	1.55	1.37	2.15	0.06	1.77
PID IMC-based	0.69	4.77	1.22	–	3.14	0.46	1.77
PIDA – Haalman	0.87	5.01	1.46	0.66	10	0.67	1.77
PID – Haalman	0.64	4.12	1.03	–	10	1.29	1.78

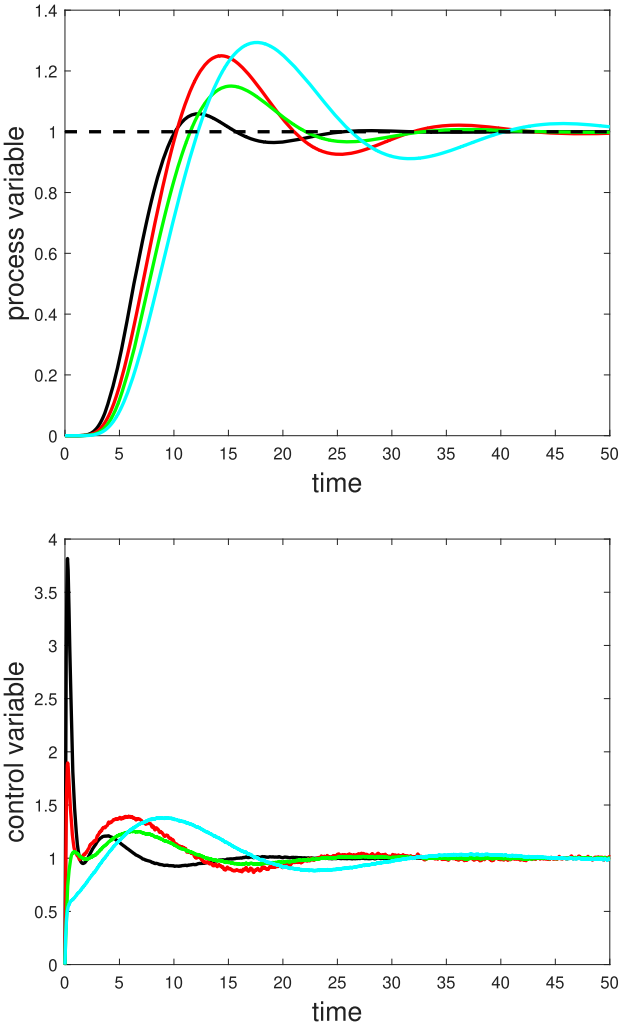

Figure 11. Set-point step responses for Example 2. Top: process variable. Bottom: control variable. Black line: IMC-based PIDA controller. Green line: IMC-based PID controller. Red line: PIDA controller tuned with the generalised Haalman method. Cyan line: PID controller tuned with the generalised Haalman method.

the set-point step response and of 30% for the load disturbance step response, while the TV is reduced of 29% and 80%, respectively.

Table 4. Controller parameters for different values of r for Example 1.

Value of r	K_p	T_i	T_d	T_a	N	M_s	IAE_{sp}	TV_{sp}	IAE_{ld}	TV_{ld}
3	1.17	3.09	0.70	0.45	1.05	1.55	2.75	7.32	2.62	1.10
4	0.87	2.81	0.46	0.39	0.33	1.60	3.40	1.86	3.22	1.13
5	0.66	2.52	0.17	0.23	0.04	1.58	4.14	1.50	3.81	1.17

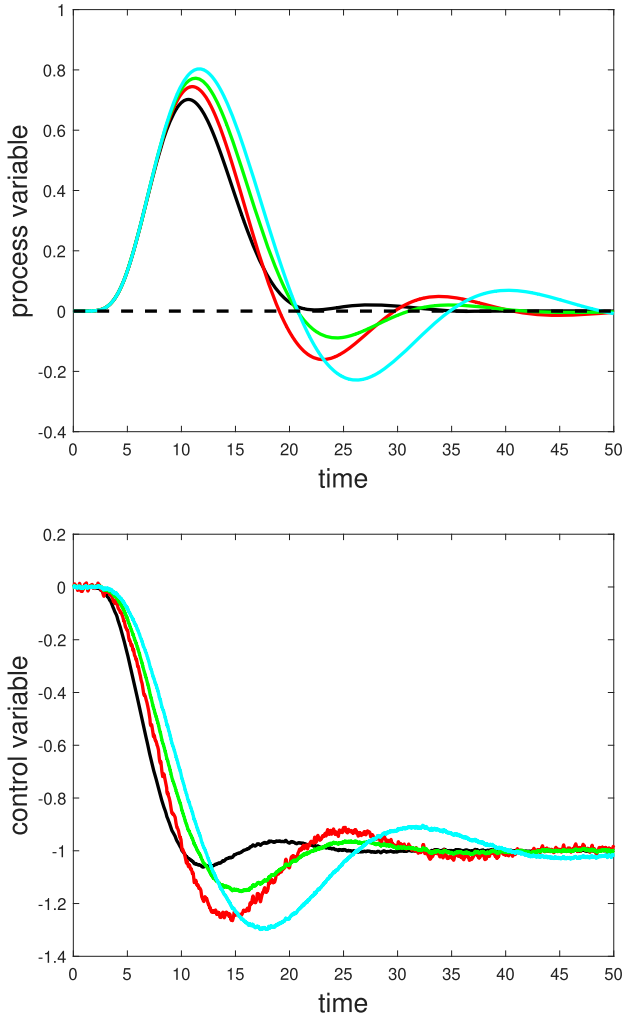

Figure 12. Load disturbance step responses for Example 2. Top: process variable. Bottom: control variable. Black line: IMC-based PIDA controller. Green line: IMC-based PID controller. Red line: PIDA controller tuned with the generalised Haalman method. Cyan line: PID controller tuned with the generalised Haalman method.

5. Experimental results

The PIDA controller has been tested in a temperature control problem by means of the APMonitor Temperature Control Lab (APMonitor, 2016). This is a take-home kit where the temperature of a transistor can be controlled by varying the current through it. The temperature is measured by means of a thermistor and both the actuator and the sensor are connected to an Arduino board. The controller has been implemented in Simulink, exploiting available libraries, with a sampling period of 0.05 s. In order to make the control task more challenging, an additional dead time of 20 s has been implemented via software.

It has to be stressed that the process is not of high order, so that the practical benefit of a PIDA controller over a PID one is limited. Nevertheless, this experimental results are meaningful as, in any case, they show the applicability of the PIDA controller and its tuning in a practical context, in particular with a significant measurement noise.

Table 6. Performance indexes obtained for Example 2.

Controller	IAE_{sp}	TV_{sp}	IAE_{ld}	TV_{ld}
PIDA IMC-based	6.91	8.31	6.45	2.13
PID IMC-based	10.2	11.7	9.19	10.9
PIDA – Haalman	10.3	8.85	8.96	6.49
PID – Haalman	12.5	14.2	11.1	13.7

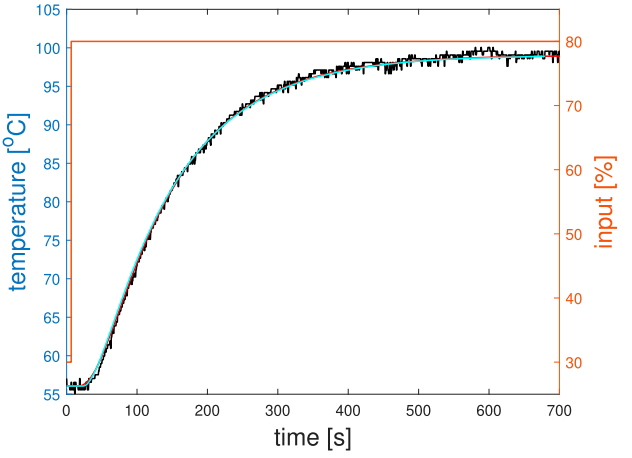

Figure 13. The experimental open-loop step response. Black line: process variable. Red line: step response of $P_{to}(s)$. Cyan line: step response of $P_{so}(s)$.

First, an input step from 30% to 80%, starting from steady-state conditions, has been applied to the process in order to estimate the process model. The open-loop step response result is shown in Figure 13. The estimated parameters of the TOPDT model are $K = 0.86$, $\theta = 46.51$, $\alpha = 0.2933$, $\tau = 111.89$, which implies that the TOPDT process transfer function can be written as

$$P_{to}(s) = \frac{0.86}{3022s^3 + 3948s^2 + 144.8s + 1} e^{-13.6s}. \quad (24)$$

On the other side, the second-order transfer function, estimated by applying the iterative method proposed in Veronesi et al. (2024) for the purpose of tuning a PID controller, results as

$$P_{so}(s) = \frac{0.86}{2292s^2 + 134.4s + 1} e^{-23.7s}. \quad (25)$$

The step responses of the two models are also shown in Figure 13, where it appears that they are almost overlapped, confirming that the process dynamics is actually of second order.

Then, by selecting $r = 3$ and $\lambda = 25$, the IMC-based tuning procedure can be applied, yielding the PIDA

Table 7. Results obtained for temperature control problem.

Controller	K_p	T_i	T_d	T_a	N	T_f	M_s	IAE_{sp}	TV_{sp}	IAE_{ld}	TV_{ld}
PIDA IMC-based	1.41	124.7	10.1	22.6	0.62	5.16	1.34	2231	55.2	1482	34.7
PID IMC-based	1.20	118.2	1.70	–	0.014	5.72	1.34	2635	49.0	1771	24.4
PIDA – Haalman	1.86	144.8	27.3	208.8	10	6.27	1.34	1964	190.3	1432	136.0
PID – Haalman	2.03	134.4	17.1	–	10	15.32	1.34	1808	204.0	1411	329.4

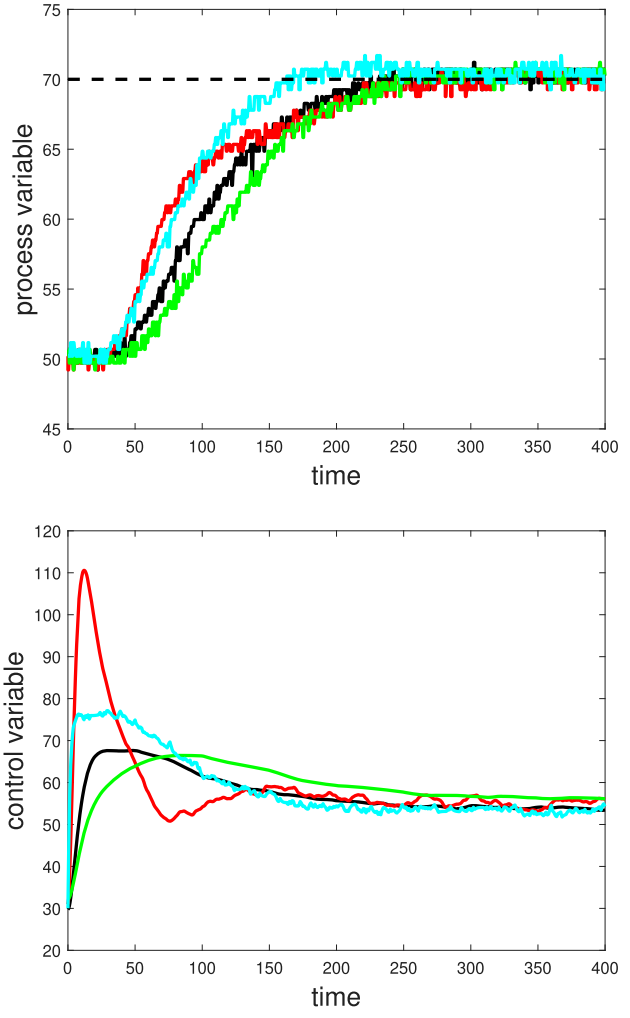

Figure 14. Set-point step (from 50 to 70°C) responses for the temperature control problem. Top: process variable. Bottom: control variable. Black line: IMC-based PIDA controller. Green line: IMC-based PID controller. Red line: PIDA controller tuned with the generalised Haalman method. Cyan line: PID controller tuned with the generalised Haalman method.

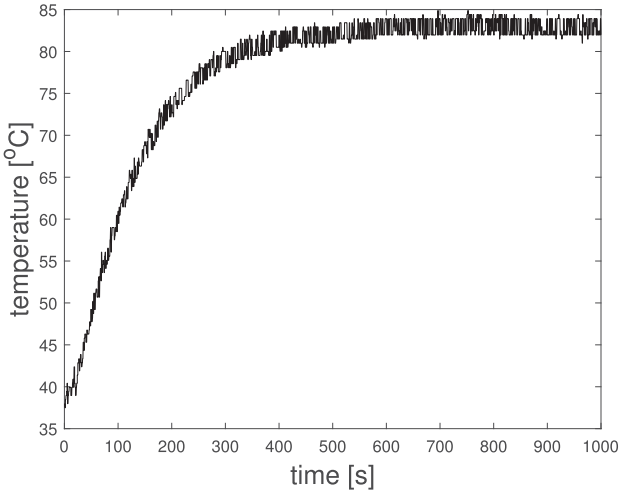

Figure 15. Temperature increment of the second heater used as a load disturbance.

(and PID) parameters shown in Table 7, where also the parameters obtained by applying the generalised Haalman tuning are shown. The filter time constants have been selected in order to have a similar (strong) noise filtering for all the controllers. The resulting set-point step responses (from 50°C to 70°C) are shown in Figure 14. It can be observed that the controllers tuned with the Haalman method provide a slightly smaller IAE at the expense of a bigger control effort. The IMC-based PIDA controller performs slightly better than the corresponding PID one, although, in general, results are comparable. It is in any case worth stressing that the control variable for the IMC-based PIDA controller is not noisy and there is no kick at the beginning of the transient, so that it is not detrimental for the actuator. On the other side, the Haalman tuning provides for the PIDA controllers a more aggressive control action with a large initial amplitude that yields a saturation of the actuator (note that in the figure, the controller output is plotted, but the actual process input is limited to 100%).

Load disturbance responses have been obtained by driving the output at the steady-state value of 50°C and then by applying a 100% input to the other heater of the system, which is next to the one considered in the control problem. It has to be noted (see Figure 15) that the actual load disturbance is not a step, and therefore there are not big differences between the step responses. The load disturbance responses are plotted in Figure 16.

Similar considerations to the set-point following task results can be done also in this case related to load disturbance: thanks to the appropriate design of the low-pass filters, the IMC-based PIDA controller (as well as the IMC-based PID controller) do not cause any problem with the noise. On the other side, the Haalman tuning with the (double) derivative filter parameters fixed to 10 provides a slightly better response but this is paid by a

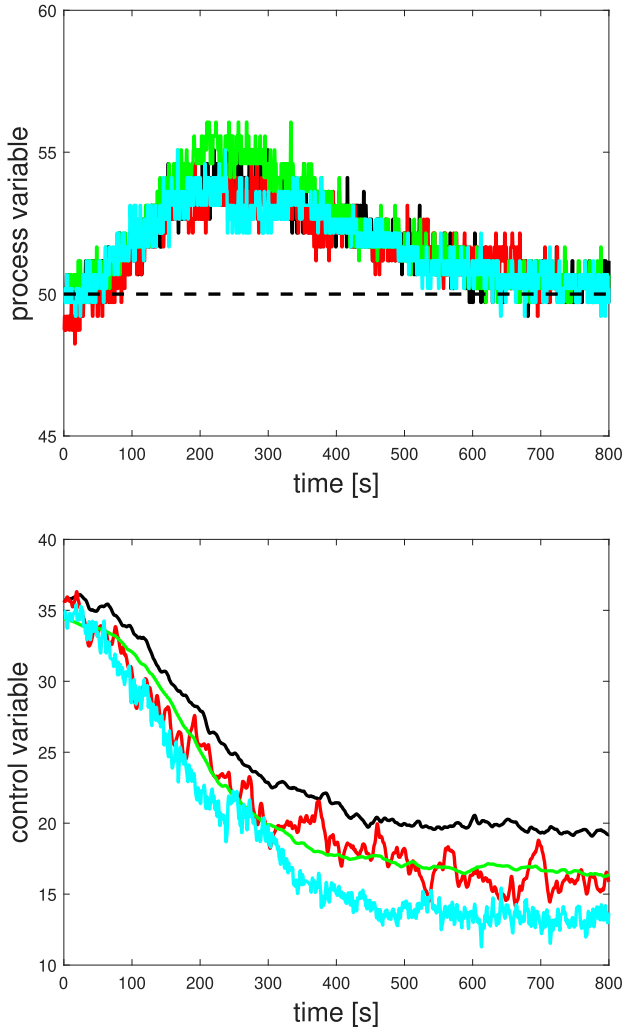

Figure 16. Load disturbance responses for the temperature control problem. Top: process variable. Bottom: control variable. Black line: IMC-based PIDA controller. Green line: IMC-based PID controller. Red line: PIDA controller tuned with the generalised Haalman method. Cyan line: PID controller tuned with the generalised Haalman method.

higher noise amplification, although higher values of the filter time constants have been selected.

Once again, it has to be stressed that the aim of these experiments is not to show the superiority of the PIDA controller with respect to the PID one, since the process is not of high order, but to show the applicability of the PIDA controller in a real application and the effectiveness of the proposed tuning methodology.

6. Conclusions

In this paper, we have proposed an IMC-based tuning methodology for PIDA controllers that exploits a process model obtained by evaluating an open-loop step response. Simulation results have shown that the PIDA controller is capable to improve the performance of a PID controller tuned by using the same approach and achieving the same robustness level, without any detrimental effect in the control variable, thanks to the use of properly designed low-pass filter. Experimental results have also demonstrated that the noise amplification and the double derivative kick are not an issue from a practical point of view thanks to the integrated design of the low-pass filters employed in the controller. The method represents a valid alternative to the generalised Haalman method based on pole-zero cancellation for the control of high-order processes and, in general, confirms the soundness of providing efforts in the investigation of controllers with high-order derivatives for industrial processes.

Future work will include a thorough comparison of the proposed method with other PID tuning methodologies and the development of rules for the automatic selection of the design parameters. Further, the extension of the proposed method to controllers with higher-order derivatives (i.e. including the jerk action Huba & Vrancic, 2021) will also be investigated.

Disclosure statement

No potential conflict of interest was reported by the author(s).

Funding

Project co-funded by the European Union – Next Generation Eu - under the National Recovery and Resilience Plan (NRRP), Mission 4 Component 1 Investment 4.1 – Call for tender No. 2333 (22nd December 2023) of Italian Ministry of University and Research; Concession Decree No. 118 (2nd March 2023) adopted by the Italian Ministry of University and Research, Project code D93C23000450005, within the Italian National Program PhD Programme in Autonomous Systems (DAuSy).

References

APMonitor (2016). *Temperature control lab*. Retrieved September 5, 2025, from https://apmonitor.com/pdc/index.php/Main/ArduinoTemperatureControl

Aryan, P., Kumar, V., Raja, G. L., Chelliah, T. R., & Hote, Y. V. (2025). Robust shifted-IMC based modified decoupled Smith predictor for delay-dominant integrating-type chemical processes. *International Journal of Systems Science*, *57*(3), 740–758. https://doi.org/10.1080/00207721.2025.2510313

Åström, K. J., & Hägglund, T. (2000). Benchmark systems for PID control. In *Preprints IFAC workshop on digital control PID'00* (pp. 181–182). Pergamon.

Åström, K. J., & Hägglund, T. (2006). *Advanced PID control*. ISA Press.

Bistak, P., Huba, M., Vrancic, D., & Chamraz, S. (2023). IPDT model-based Ziegler–Nichols tuning generalized to controllers with higher-order derivatives. *Sensors*, *23*(8), 3787. https://doi.org/10.3390/s23083787

Biswas, B., Chakrabarti, A., & Raja, G. L. (2025). Indirect IMC-PID controller for a DC-DC boost converter. In *Proceedings of the International Conference on Systems, Control and Automation* (pp. 29–43). Springer.

Bošković, M. Ç., Šekara, T. B., & Rapaić, M. R. (2020). Novel tuning rules for PIDC and PID load frequency controllers considering robustness and sensitivity to measurement noise. *International Journal of Electrical Power & Energy Systems*, *114*, Article 105416. https://doi.org/10.1016/j.ijepes.2019.105416

Campregher, F., Milanesi, M., Schiavo, M., & Visioli, A. (2024). Generalized Haalman tuning of PIDA controllers. In *Proceedings IFAC Conference on Advances in PID Control* (pp. 406–411). Elsevier.

Ferrari, M., & Visioli, A. (2022). A software tool to understand the design of PIDA controllers. In *Proceedings IFAC Symposium on Advances in Control Education*. Elsevier.

Huba, M. (2019). Filtered PIDA controller for the double integrator plus dead time. In *Proceedings 16th IFAC Conference on Programmable Devices and Embedded Systems* (pp. 106–113). Elsevier.

Huba, M., Bistak, P., Brieznik, J., & Vrancic, D. (2024). Constrained series PI, PID and PIDA controller design inspired by Ziegler–Nichols. *Power Electronics and Drives*, *9*(1), 331–346. https://doi.org/10.2478/pead-2024-0021

Huba, M., Bistak, P., & Vrancic, D. (2023a). Parametrization and optimal tuning of constrained series PIDA controller for IPDT models. *Mathematics*, *11*(20), 4229. https://doi.org/10.3390/math11204229

Huba, M., Bistak, P., & Vrancic, D. (2023b). Series PIDA controller design for IPDT processes. *Applied Sciences*, *13*(4), 2040. https://doi.org/10.3390/app13042040

Huba, M., & Vrancic, D. (2021). Extending the model-based controller design to higher-order plant models and measurement noise. *Symmetry*, *13*(5), 798. https://doi.org/10.3390/sym13050798

Kumar, M., & Hote, Y. V. (2021). PIDD2 controller design based on internal model control approach for a non-ideal DC-DC boost converter. In *2021 IEEE Texas Power and Energy Conference (TPEC)* (pp. 1–6). IEEE.

Milanesi, M., Mirandola, E., & Visioli, A. (2022). A comparison between PID and PIDA controllers. In *Proceedings 27th International Conference on Emerging Technologies and Factory Automation*. IEEE.

Milanesi, M., Visioli, A., & Chen, Y. Q. (2025). From PID to PIDD$^{2\alpha}$: Performance improvement with a fractional double derivative action from PID to PIDD$^{2\alpha}$: Performance improvement with a fractional double derivative action. *Annual Reviews in Control*, *60*, Article 101006. https://doi.org/10.1016/j.arcontrol.2025.101006

Monje, C. A., Vinagre, B. M., Feliu, V., & Chen, Y. Q. (2008). Tuning and auto-tuning of fractional order controllers for industry applications. *Control Engineering Practice*, *16*(7), 798–812. https://doi.org/10.1016/j.conengprac.2007.08.006

O'Dwyer, A. (2006). *Handbook of PI and PID tuning rules*. Imperial College Press.

Sanchez, J., Dormido, S., & Diaz, J. M. (2021). Fitting of generic process models by an asymmetric short relay feedback experiment–the n-shifting method. *Applied Sciences*, *11*(4), 1651. https://doi.org/10.3390/app11041651

Sanchis, R., & Peñarrocha-Alós, I. (2022). A new method for experimental tuning of PI controllers based on the step response. *ISA Transactions*, *128*, 329–342. https://doi.org/10.1016/j.isatra.2021.09.008

Sanchis, R., & Peñarrocha-Alós, I. (2023). Optimal tuning of PID controllers with derivative filter for stable processes using three points from the step response. *ISA Transactions*, *143*, 596–610. https://doi.org/10.1016/j.isatra.2023.10.009

Tepljakov, A., Alagoz, B. B., Yeroglu, C., Gonzalez, E., HosseinNia, S. H., & Petlenkov, E. (2018). FOPID controllers and their industrial applications: A survey of recent results. *IFAC-PapersOnLine*, *51*(4), 25–30. https://doi.org/10.1016/j.ifacol.2018.06.014

Veronesi, M., de Keyser, R., Vilanova, R., & Visioli, A. (2024). Estimation of a SOPDT process transfer function for PID tuning. In *Proceedings IFAC Conference on Advances in PID Control*. Elsevier.

Visioli, A. (2006). *Practical PID control*. Springer.

Visioli, A., & Sanchez-Moreno, J. (2023). Design of PIDA controllers for high-order integral processes. In *Proceedings 28th International Conference on Emerging Technologies and Factory Automation*. IEEE.

Visioli, A., & Sanchez-Moreno, J. (2024a). IMC-based tuning of PIDA controllers: A comparison with PID control. In *Proceedings IFAC Conference on Advances in PID Control*. Elsevier.

Visioli, A., & Sanchez-Moreno, J. (2024b). A relay-feedback automatic tuning methodology of PIDA controllers for high-order processes. *International Journal of Control*, *97*(1), 51–58. https://doi.org/10.1080/00207179.2022.2135019